J Mater Sci: Mater Med (2008) 19:937–946
DOI 10.1007/s10856-007-3222-3

Effect of ceramic conversion treatments on the surface damage and nickel ion release of NiTi alloys under fretting corrosion conditions

H. Dong · X. Ju · H. Yang · L. Qian · Z. Zhou

Received: 12 May 2006 / Accepted: 10 January 2007 / Published online: 1 August 2007

Abstract Recent researches have demonstrated that surface modification can improve the fretting wear resistance of NiTi alloys in air or enhance their aqueous corrosion resistance without fretting. However, little is known about the behaviour of surface engineered NiTi under fretting corrosion conditions. This is important for such body implants as orthodontic arch wires and orthopedic bone fixation devices because they need to withstand the combined attack of corrosion from body fluid and mechanical fretting. In this study, a NiTi alloy was ceramic conversion (CC) treated at 400 and 650 °C. The effect of the surface treatment on the fretting corrosion behaviour of NiTi alloy was investigated using fretting corrosion tests in the Ringer's solution. The experimental results have shown that the CC treatment can convert the surface of NiTi into a TiO_2 layer, which can effectively improve the fretting corrosion resistance of NiTi alloy and significantly reduce Ni ion release into the Ringer's solution. Detailed SEM observations revealed that the untreated samples were severely damaged by adhesion and delamination; the high temperature (HT) (650 °C/1 h) treated samples were damaged mainly by spallation and adhesion; and the low temperature (LT) (400 °C/50 h) treated samples were characterised by mild abrasion. Mild oxidation and corrosion were also observed for all three types of samples tested under fretting corrosion conditions.

H. Dong · X. Ju (✉)
The Department of Metallurgy and Materials, The University of Birmingham, Birmingham B15 2TT, UK
e-mail: xxj248@bham.ac.uk

H. Yang · L. Qian · Z. Zhou
Tribology Research Institute, National Traction Power Laboratory, Southwest Jiaotong University, Chengdu 610031, P.R. China

Introduction

NiTi shape memory alloys (SMAs) are attractive for medical implant applications due to their unique combination of superelasticity and shape memory effect, constant actuated force, low modulus, kink resistance, MRI (magnetic resonance imaging) compatibility and assumed biocompatibility [1, 2]. As a result, NiTi SMAs are finding an expanding number of applications, including constant corrective force orthodontic wires; devices for fracture fixation; anchoring of prostheses; treatment of scoliosis; osteosynthesis staples; aneurysm clips; intrauterine contraceptive devices; artificial heart valves; self-expandable arterial and esophageal stents; extravessel correctors and artificial muscles [3].

Notwithstanding the fact that as bulk materials NiTi SMAs are in general biocompatible due to the formation of a thin native surface oxide layer, dissolution and release of Ni ions would cause allergic, toxic and carcinogenic effects [4, 5]. For example, in vivo studies show a slower osteogenic process, inferior bone contact and lower synthesis of mineralization mediating proteins with NiTi SMAs compared with conventional titanium alloys [6]. Clearly, the biocompatibility of NiTi implants is closely related to the surface oxide films formed in the host environment and their resistance to such surface degradation as corrosion, wear or both. However, this layer is too thin (2–20 nm) to withstand the relative movement between implants and hard tissues. This is of concern particularly for such applications as bone stables, bone joints and arch wires, where small amplitude movement between bone and the implant would cause fretting corrosion. This is further complicated by the fact that NiTi repassivates much slower than Ti and Co–Cr alloys [4]. Therefore, fretting corrosion appears to be one of the major problems of the material in

these bio-tribological applications. Shear micro-movements may start just after surgery and so fretting corrosion could be suffered due to the activity of the patient [7, 8].

Surface engineering has been proved to be a key technology in addressing the above problem, and a state-of-the-art overview has been given by Hassel recently [9]. Although surface coatings such as TiN [10], hydroxyapatite [11] and diamond-like carbon [12] can, to some extent, improve the biocompatibility of NiTi SMAs, low bonding strength and deformation capacity are major concerns over these hard surface coatings. Therefore, it seems that surface modification could be a more promising surface engineering approach, and a series of surface modification techniques have been developed to form a biocompatible titanium oxide layer on the surface of NiTi SMAs based on mechanical polishing, electropolishing, anodizing, chemical passivation and thermal oxidation in air, water steams and boiling solutions [13–21]. All these treatments can form a surface oxide layer, which can reduce the corrosion and Ni ion release of NiTi alloys under corrosion conditions.

In addition to corrosion attack, some body implants also suffer from mechanical interaction with the hard tissues. However, except for thermal oxidation in air, the oxide layers formed on NiTi alloys by most of these treatments are too thin to withstand such mechanical attack. An advanced ceramic conversion technique based on thermal oxidation has recently been developed to effectively improve the tribological properties of such titanium-based alloys as Ti-6Al-4V [22] and Ti–Al intermetallics [23].

It should be pointed out that some body implants (such as arch wires and bone plates) suffer from combined attack of corrosion of body fluid and mechanical fretting. To date all in vitro studies on surface engineered NiTi have been conducted either under aqueous corrosion or dry wear conditions. For example, Tan et al. found that oxygen ion implantation can enhance the fretting wear resistance of NiTi alloy under dry conditions [24]; on the other hand, Huang et al. [25] investigated the electrochemical corrosion and Ni ion release of thermal oxidation treated NiTi alloys without mechanical interaction.

Clearly, it is a timely task to study the behaviour of surface engineered NiTi alloys under corrosion and fretting conditions from both a scientific and a clinical point-of-view. To this end, the present study was directed at investigating the fretting corrosion behaviour of untreated and ceramic conversion treated NiTi samples using a fretting wear tester in the Ringer's solution. The fretting wear and the nickel ion release were quantitatively measured, and the fretting damage was investigated using SEM/EDX. Based on the experimental results, the fretting corrosion mechanism involved was discussed.

Materials and methods

Materials and surface treatment

The material used was a NiTi shape memory alloy with a nominal composition of 44.32 wt% Ti and 55.68 wt% Ni, which was provided in annealed bar form (16 mm diameter) by Memory-Metalle GmbH, Germany. Platelet samples $20 \times 10 \times 4$ mm were cut from this bar using electrical discharge machining. Prior to surface treatment, samples were wet ground with SiC papers down to 1,200 grit and ultrasonically cleaned in acetone and dried with hot air. A series of ceramic conversion (CC) treatments were conducted through thermal oxidation in air at temperatures between 400 and 1,000 °C for 0.5–100 h. Judging from the deformation ability, surface nickel concentration and the effect on the transformation temperatures (which will be reported separately) [26], two optimal CC treatments, 400 °C/50 h(LT) and 650°C/1 h(HT), were selected for further detailed fretting corrosion investigation.

General characterisation

Phase identification was carried out with an X-ray diffractometer (X'Pert, Philips, Netherland) using Cu-Kα radiation (wavelength 0.1542 nm). Surface treated samples were cross-sectioned normal to the surface, mounted in bakelite and wet ground with emery papers from 240 down to 1,200 grit. After polishing, the samples were etched in a solution consisting of 40%HF, 70% HNO_3 and H_2O in the ratio of 1:3:6. The cross-sectional microstructures of the treated specimens were examined using a field emission SEM (JSM-7000F, JEOL, Japan). The bonding of the surface ceramic layer to the substrate and the load bearing capacity of the ceramic conversion treated samples were studied by scratch tests using a friction monitored scratch tester (ST 3001, Teer Coatings, UK).

Fretting corrosion tests

In order to simulate the service conditions of some SMA implants under fretting and corrosion conditions, fretting corrosion tests were carried out on a horizontal servo-hydraulic fretting test machine (DS20, PLINT, France) as described elsewhere [27]. 1Cr13 (AISI 420) martensitic stainless steel balls (40 mm diameter) with a surface roughness of 0.1 μm (R_a) were used to fret against flat NiTi plate samples since they are corrosion resistant and nominally contain no nickel. During the tests, the plate was stationary and the 1Cr13 ball reciprocates horizontally. The normal load (F_n) used was 100 N and the fretting frequency was selected as 5 Hz. The displacement amplitude was kept constant: D = 100 μm. The number of fretting

cycles chosen was 10,000, 20,000 and 50,000. All tests were performed in a 150 ml Ringer's solution (1.1250 wt% NaCl, 0.0525 wt% KCl, 0.0315 wt% $CaCl_2$, 0.0250 wt% $NaHCO_3$ and balance water) at room temperature and at each condition the fretting tests were repeated at least twice.

Post-test analysis

After the fretting corrosion tests, the nickel ion concentration in the Ringer's solution was determined by a Spectra Atomic Absorption Spectrometer (VARIAN, USA). The depth profiles of the fretting craters were measured using a profilometer (Surfcorder SE 1700, Metrology International, UK). The surface morphologies of the fretting wear scars were examined using a field emission SEM (JSM-7000F, JEOL, Japan) equipped with an energy-dispersive X-ray (EDX).

Statistic analysis

The amount of Ni ion release into the Ringer's solution during the fretting corrosion tests were statistically analysed using *t*-Student tests. Differences are reported as significant for $p < 0.01$. Data are presented in bar chart and expressed as the mean ± standard deviation.

Results

Surface layer characteristics

The XRD spectra of untreated (UT) and 400 °C/50 h (LT) and 650 °C/1 h (HT) treated NiTi samples are given in Fig. 1, showing austenite (B2) in conjunction with small amount of martensite (B19') as the main constituent phases in the as-received NiTi samples. It can be seen from Fig. 1 that both anatase and rutile TiO_2 formed during 400 °C/50 h treatment. In addition, the relative intensity of the martensite was increased slightly although the B2 phase still dominates. This implies that the treated surface layer is very thin and so the X-ray can penetrate into the substrate. The XRD spectrum for the 650 °C/1 h is quite different from that for 400 °C/50 h treated samples. As can be seen from Fig. 1, when treated at 650 °C, rutile became the dominant form of TiO_2, and Ni_3Ti and Ni phases were also formed during the treatments. The peaks from the substrate can still be observed but with a significantly decreased intensity, indicating that much thicker surface layers were formed.

The cross-sectional microstructures of the LT and HT samples are given in Figs. 2 and 3a, respectively. It can be seen that after 400 °C/50 h treatment, a very thin (<1 μm) layer was formed on the surface (Fig. 2). However, after 650 °C/1 h treatment, two distinct layers were produced on the surface (Fig. 3a). An EDX line scanning across the treated layer was conducted, and the results are shown in Fig. 3b. It seems that the outer layer was rich in O and Ti and lean in Ni while the inner layer was rich in Ni and lean in Ti and O. Therefore, based on the XRD spectrum (Fig. 1), EDX scan (Fig. 3b) and SEM microstructure (Fig. 3a), it could be deduced that the surface modified case of the HT samples consisted of a top TiO_2 enriched layer followed by an inner Ni_3Ti enriched layer. This has been further conformed by quantitative EDX dot analysis results (Table 1).

Scratch behaviour

Scratch tests were carried out to assess the quality of the modified layers and the interfacial bonding strength. The

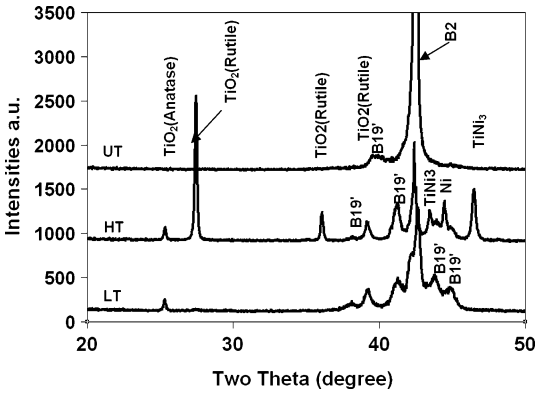

Fig. 1 XRD spectra of NiTi samples (UT: untreated, LT: 400 °C/50 h and HT: 650 °C/1 h). For clarity, the XRD profiles for LT, HT and UT are shifted to higher intensities by 100, 900 and 1,700, respectively

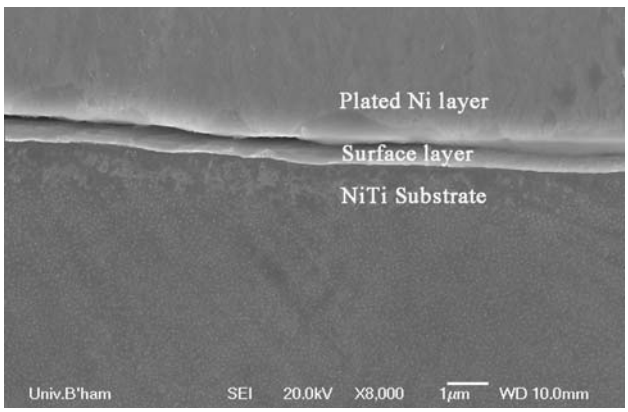

Fig. 2 The SEM cross-section structure of the 400 °C/50 h treated sample

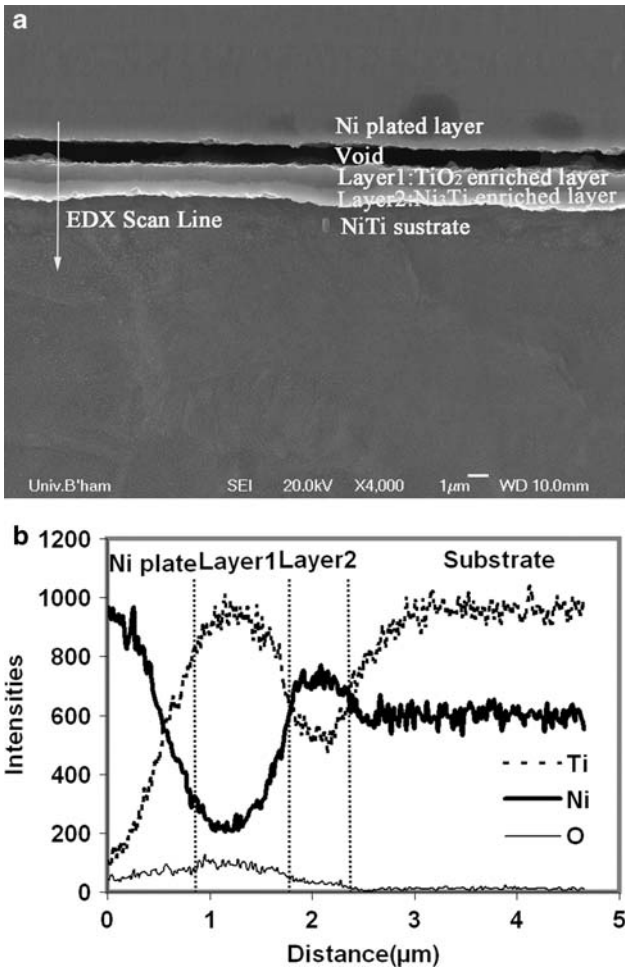

Fig. 3 (**a**) The SEM cross-section structure (**b**) EDX line scan across the surface layer of the 650 °C/1 h treated sample

Table 1 EDX dot analysis results

	O (at%)	Ti (at%)	Ni (at%)	Possible phases
Outer layer	69.5	30.3	0.2	TiO_2 +Ni
Inner layer	0	26.3	73.7	Ni_3Ti
Substrate	0	49.1	50.9	NiTi

friction force and its first derivative against the scratch load for the LT and HT samples are shown in Figs. 4a, b respectively. It can be seen that in general the friction force increased with the applied load. Although the fluctuation of the 1st derivative of friction force increased with the load during the scratch process for the LT sample, no sudden jump in the friction force was observed until a high load of about 90 N was reached (Fig. 4a). This implies that damage of the surface layer may have occurred but the interfacial bonding between the surface modified layer and the substrate was not removed. This was further confirmed by the SEM observations of the scratch track. No obvious damage occurred in the majority of the track and near the

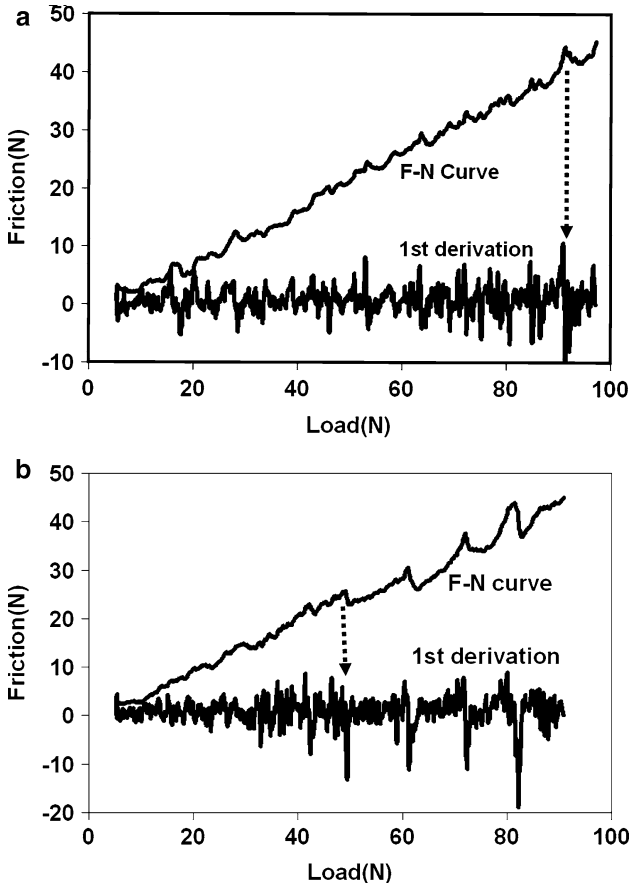

Fig. 4 The friction force and its first derivation against scratch load for (**a**) 400 °C/50 h and (**b**) 650 °C/1 h treated samples

end of the scratch track the surface layer was removed and the substrate was exposed. Typical conformal crack morphologies appeared in the track, indicating that the modified layer has very good deformation compatibility and the bonding of the surface layer to the substrate is very good [28].

In contrast, for the HT samples a sudden increase in friction force was observed at a normal load of about 50 N (Fig. 4b), followed by several larger sudden jumps observed on the friction and 1st derivative curves. This means that the surface oxide layer of the HT sample was damaged at a much lower load as compared with that (90 N) for the LT samples (Fig. 4a). SEM observations of the scratch track revealed buckling and spalling in the track and recovery spallation on the edges at an early stage under a light load. Toward the end of the scratch, more and more severe buckling and spallation occurred in the track and along the edges, and finally the substrate was almost completely exposed with the surface oxide layer being entirely removed. Clearly, the surface oxide layer formed on the HT samples is more brittle and the bonding strength is much lower relative to that on the LT samples.

The fretting kinetic behaviour

Figure 5 plots the real time evolution of the friction force (F_t) as a function of the number of cycles (N) and fretting displacement (d) of the untreated and ceramic conversion treated NiTi samples against 1Cr13 steel ball in the Ringer's solution up to 20,000 cycles. It can be seen that all the friction force versus displacement (F_t–D) curves remain open and finally stable in parallelogram shape, which is characteristic of the gross slip regime. Experimental results revealed that under the experimental conditions all the untreated and surface treated samples were in gross slip regime up to 50,000 cycles.

In addition to the frictional logs, the F_t–N curves also provide important information on the fretting kinetics. The evolution of the friction force against the number of cycles up to 20,000 cycles is summarised in Fig. 6. At the beginning, all the F_t–N curves showed an increase in F_t, which can be explained as the removal of the contamination on the surface and the increase in contact area of samples [29]. For untreated samples, after about 20 cycles F_t reached a plateau and then reduced gradually before it increased again at about 3,000 cycles (Fig. 6). Eventually, F_t reached another plateau with some fluctuation during the later stage from 10,000 to 50,000 cycles.

The F_t–N curves for both the LT and HT samples are similar within the first 100 cycles. The F_t increased with the fretting cycles but the value is much lower than that of the untreated material, indicating the friction-reduction function of the surface oxide layer formed by the CCT. Then significant difference in F_t was observed between the HT and LT samples: while the F_t for the LT sample started to reduce with the cycles after peaking at about 100cycles, the F_t for the HT samples still kept increasing further with the cycles until it was peaked after about 3,000 cycles. Large fluctuation in F_t for the HT samples was observed as well in the period from 200 to 3,000 cycles. Compared with the F_t for the LT sample, which retained relatively stable right after about 3,000 cycles, the F_t for the HT did not reach a relatively stable stage until about 7,000 cycles. The untreated sample also maintained relatively stable after about 7,000 cycles, and it showed a very similar stable F_t to that for the HT sample. However, the LT samples demonstrated the lowest and stablest friction force (F_t) among all the three types of samples.

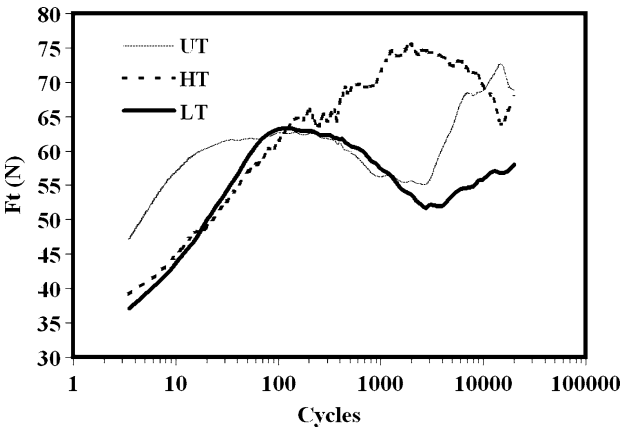

Fig.6 The F_t –N curves of the untreated and surface treated samples (UT: untreated, LT: 400 °C/50 h and HT: 650 °C/1 h)

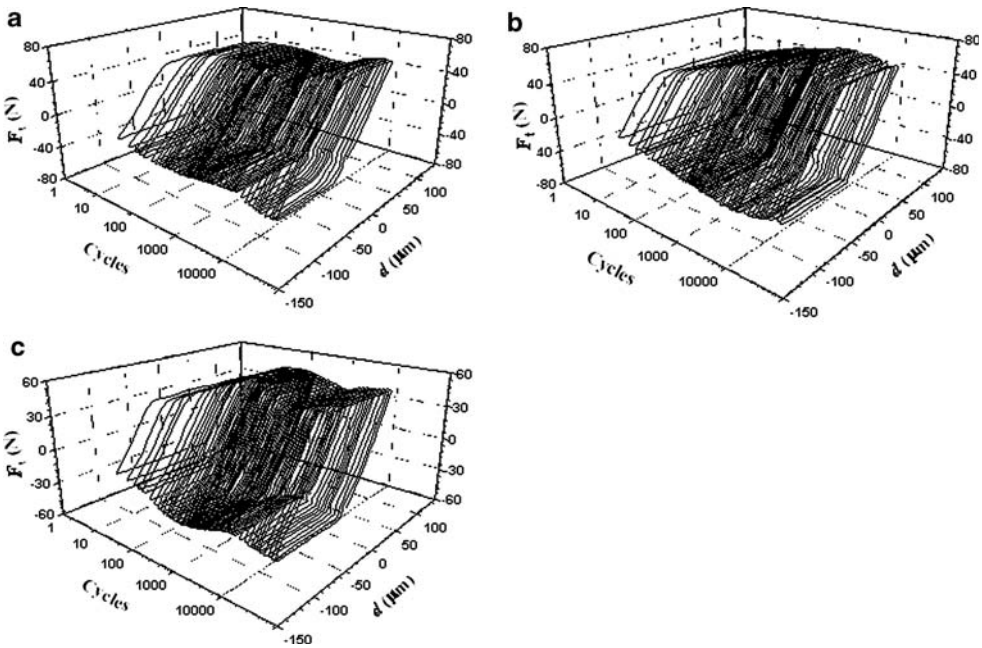

Fig. 5 The frictional logs (F_t–d–N curves) of (**a**) untreated and (**b**) 650 °C/1 h and (**c**) 400 °C/50 h treated samples against 1Cr13 steel ball up to 20,000 cycles

Nickel release during fretting wear

Following the fretting corrosion tests, the nickel ion concentration in the Ringer's solution was measured using an atomic absorption spectrometer to monitor the release of nickel ion into the solution. As shown in Fig. 7, the concentration of nickel ions in the Ringer's solution for the untreated NiTi samples increases slowly within the first 20,000 cycles and then increase quickly from 20,000 to 50,000 cycles.

In contrast, all the surface treatments can effectively prevent the release of nickel ions from the NiTi fretting surfaces (Fig. 7). The release of nickel ions from the tested HT sample surface increased very slowly with the fretting cycles. After 50,000 fretting cycles, the maximum release of nickel ions was reduced from about 65 μg/l for the untreated UT sample to about 10 μg/L for the HT sample, representing a reduction of 85% in nickel ion release. Although the initial release of nickel into the solution after 10,000 cycles is slightly lower for the HT sample than for the LT sample, there is almost no appreciable increase in nickel release from the LT samples up to 50,000 cycles. Therefore, after 50,000 fretting cycles the LT samples produced the lowest nickel concentration in the solution, which is in good agreement with the fretting damage results given in the next section.

Fretting damage

The evolution of the fretting wear scars with the fretting cycles is demonstrated in Fig. 8 and the corresponding wear scar areas are plotted against the number of cycles in Fig. 9a. In general, the surface area of wear scars in all three types of samples increased with increasing the fretting cycles. However, the area of the wear scar in the untreated samples increased very quickly with the fretting cycles. In contrast, the surface treated samples showed a slower increase in wear scar areas. After 50,000 cycles, the wear scar area was in the following order: LT < HT < UT.

The depth profiles of the fretting craters measured by a profilometer provided supplementary information of the fretting damage. The largest depth of the fretting craters is depicted against the fretting cycles in Fig. 9b. It can be seen that the maximum depth of the fretting craters was maintained almost constant for the LT samples. On the other hand, for both the UT and HT samples the maximum depth of fretting craters first increased rapidly up to about 20,000 cycles and then reduced gradually with the fretting cycles.

Judging by both the fretting scar area and fretting craters depth, it thus follows that the LT sample showed the least fretting damage among all the three types of samples tested although no direct measurements were made of the wear volume of the fretting craters. Slight improvement in fretting damage resistance was observed for the HT samples as compared with the untreated (UT) samples.

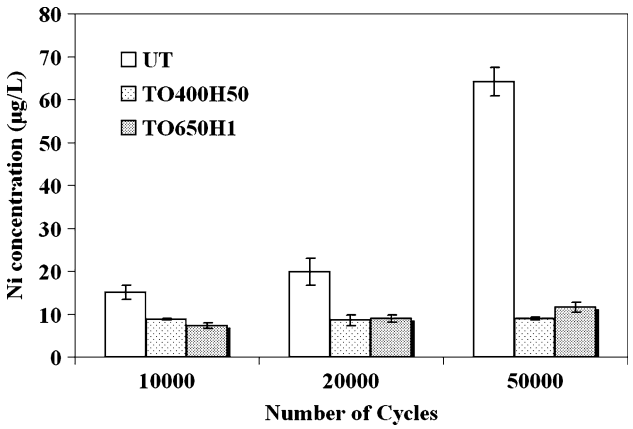

Fig. 7 The nickel concentration in the Ringer's solution used for the three types of samples plotted as a function of fretting cycles (UT: untreated, LT: 400 °C/50 h and HT: 650 °C/1 h)

Discussion

Fretting damage mechanisms

According to modern fretting theory [30], there may be three fretting regimes: (1) partial slip regime, (2) gross slip regime and (3) mixed regime. The frictional logs in Fig. 5 have indicated that under present test conditions fretting of all the samples is in the gross slip regime since all the F_t–D–N remained open and in parallelogram shape. Generally severe fretting damages would occur in this regime.

Un-treated material

As shown in Fig. 10, parallel abrasive marks along the fretting direction are distributed across the whole fretting wear scars, and adhesive wear and plastic deformation were observed in the centre of the fretting scar (Fig. 10a). The corresponding backscattered electron image (BEI) revealed black areas and cracks perpendicular to the fretting direction (Fig. 10b). Abrasion, adhesion and microcracking are the characteristic features of the gross slip regime [8].

As can be seen in Fig. 6, the friction force (F_t) increased steadily within the first 20 cycles. This could be due to the removal of the natural contaminated layers, direct asperity contact and thus adhesion occurred between the NiTi and 1Cr13 contact surfaces [31]. Because the fretting occurred in the gross slip regime, the adhesion junctions were sheared, torn away [32] and finally transferred onto the

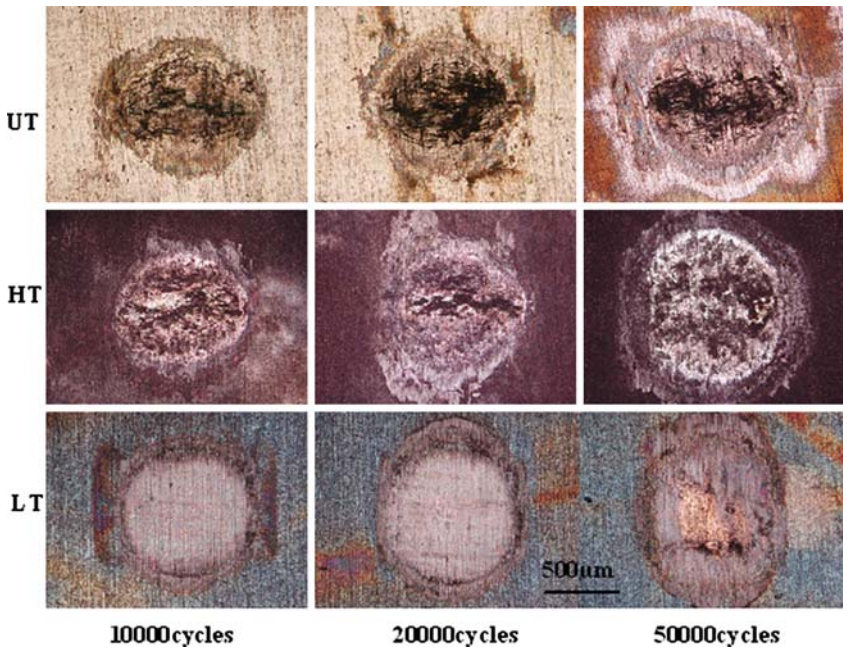

Fig. 8 The surface images of the fretting wear scars as a function of the fretting cycles (UT: untreated, LT: 400 °C/50 h and HT: 650 °C/1 h)

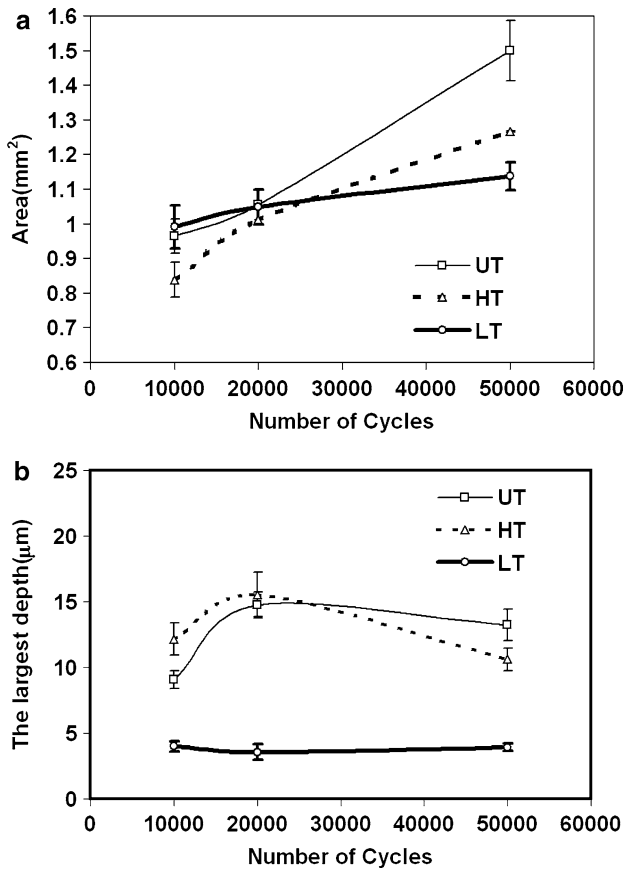

Fig. 9 The area and large depth of the wear scars plotted against the number of cycles (UT: untreated, LT: 400 °C/50 h and HT: 650 °C/1 h)

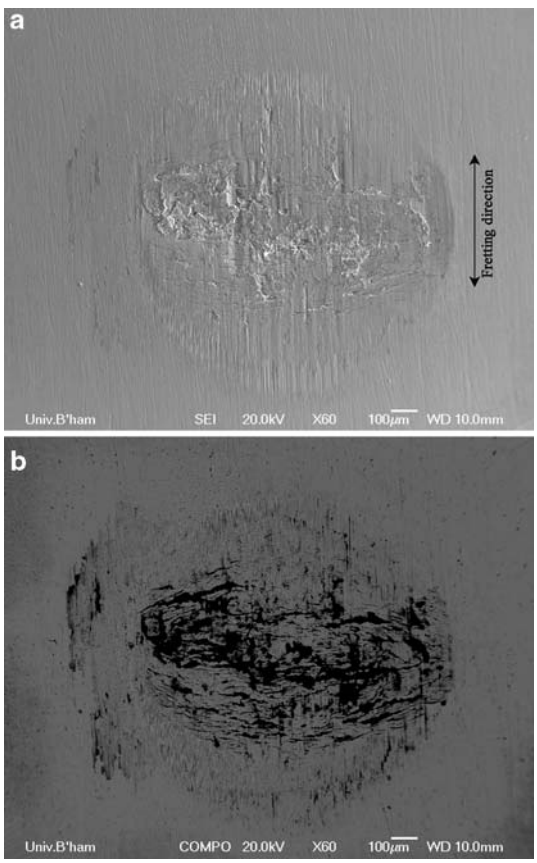

Fig. 10 SEM Fretting wear morphologies of the untreated NiTi against 1GCr13 after 5 × 104 cycles: (**a**) secondary electron image (SEI); (**b**) backscattering electron image (BEI)

counterface. The coefficient of friction increases significantly in this section owing to adhesion and plastic deformation. At the same time, work hardening, embrittlement and fracture of adhesion junctions led to the formation of metallic wear debris [29]. More and more wear debris were formed and oxidized or corroded during the fretting process, thus resulting in three-body contact and friction plateau in Fig. 6. As a result, hard oxidized wear debris would cause abrasive wear as evidenced in Fig. 10. The materials transfer and oxidation are confirmed by the X-ray mapping of the fretting scar on NiTi.

In addition, micro-cracks perpendicular to the sliding direction and localised spallation were also observed in the fretting scar. This is probably because the superficial layer of the wear surface was work hardened but embrittled by the severe plastic deformation; this layer was then cracked under the tangential friction force and delamination occurred by the connection of the horizontal cracks beneath the hardened layer. It should be indicated that corrosion by Ringer's solution is also occurred as evidenced by the Cl and Ca peaks in the EDX spectrum and Ca mapping. This is because when the naturally formed passivation oxide layer was removed by the fretting action of the 1Cr13 ball, corrosion would occur especially when the surface layer was cracked.

The CCT treated material

Both the LT and HT samples showed very similar F_t–N features within the first 100 cycles (Fig. 6), and within the first tens of cycles the F_t is lower for the surface treated LT and HT samples than for the untreated UT sample. It is possible that before the serious adhesion occurs, the surface TiO_2 oxide layer can protect the substrate and reduce friction because of its lubricious nature [22]. However, whilst the F_t for the LT samples peaked after about 100 cycles and then reduced rapidly to a stable value, the F_t for the HT samples peaked after a couple of thousand cycles (Fig. 6). Clearly, different damage mechanisms operated in these two different types of samples.

As has been shown in Fig. 8, fretting damage was observed in the HT treated samples after 10,000 cycles and the size of the wear scar increased with increasing fretting cycles. Close examination also revealed that when fretted by a 1Cr13 ball, the oxide layers formed on the HT samples were removed and the substrate of the NiTi alloy was entirely exposed. Around the rim of the fretting scar, spallation of the surface oxide layer occurred. This implies that the bonding between the surface oxide layer and the subsurface in the HT samples is poor, which is supported by the scratch test results of the HT sample (Fig. 4b). The oxide layers formed are brittle and the interfacial bonding between the oxide layer and the substrate is quite weak (Fig. 4b). Therefore, spallation of the low adherent oxide layer occurred (Fig. 11b); once the surface oxide layer was removed, direct contact and adhesion between the 1Cr13 ball and the HT sample surface may have occurred. This is in line with the high friction force (Fig. 6) and the rough central damaged areas (Fig. 11a). It thus follows that unlike the untreated samples the fretting morphologies of the HT samples are characterised by large area spallation of the surface oxide layers and severe damage in the centre areas.

The LT sample possesses the best fretting wear performance and totally different fretting mechanisms. As has been shown in Fig. 8, after 20,000 fretting cycles, no severe fretting damage observed except for several small scratches. The LT sample surface was still covered by a protective, low-friction oxide layer, and therefore low F_t is expected (Fig. 6). This is in line with the excellent scratch behaviour as shown in Fig. 4a. No adhesive wear was found on either the LT sample surface (Fig. 8) or the matching 1Cr13 ball surface. Therefore, mild abrasive wear is the dominating damage mechanism in the LT samples. Only after 50,000 cycles, some surface damages were found in the central area of the LT sample surface (Fig. 12). However, compared with the other samples

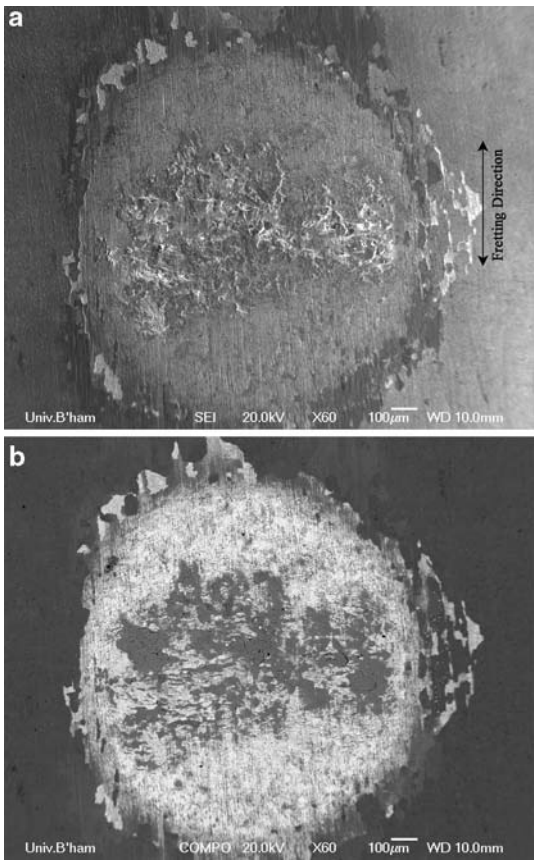

Fig. 11 SEM micrographs showing the fretting scars for the 650 °C/1 h treated NiTi sample after 50,000cycles: (**a**) SEI and (**b**) BEI

tested under the same conditions, the LT sample still shows the mildest fretting damage (Fig. 9). Therefore, the good fretting corrosion resistance of the LT samples can be attributed to the adherent and ductile surface oxide layer formed during the low-temperature ceramic conversion treatment.

The effect of surface treatment on Ni ion release

As an implantable material, the exposure of NiTi alloy can have adverse effects on human health [33]. For instance, nickel allergy in the form of contact dermatitis is the most common and well-known reaction. The accumulation of nickel in the body through chronic exposure can lead to lung fibrosis, cardiovascular and kidney diseases [34]. Therefore, it is crucial to prevent the release of nickel ion from NiTi body implants.

The experimental results (Fig. 7) have demonstrated that the nickel ion release during the fretting corrosion of NiTi against a 1Cr13 martensitic stainless steel ball in the Ringer's solution can be significantly reduced from 65 μg/L for the untreated NiTi to about 10 μg/L for the optimally surface engineered material. The reasons for this effectively reduced release of nickel ions could be twofold. First, as discussed in the preceding section, both surface treatment can improve the resistance of NiTi to fretting corrosion in terms of reduced surface area and the maximum depth of the fretting scars (Fig. 8). As a result, less wear debris was formed during the fretting corrosion process, and in turn less release of nickel ion into the Ringer's solution is expected. Second, the formation of surface TiO_2 oxide layer can effectively push nickel into the subsurface. Therefore, the wear debris formed from the surface treated samples contained less nickel, which should have also contributed to the reduced nickel ion concentration in the Ringer's solution. This is supported by the fact that although the fretting wear is more severe for the HT sample than for the LT sample (i.e., more wear debris formed), the difference in nickel ion release between these two is not statistically significant.

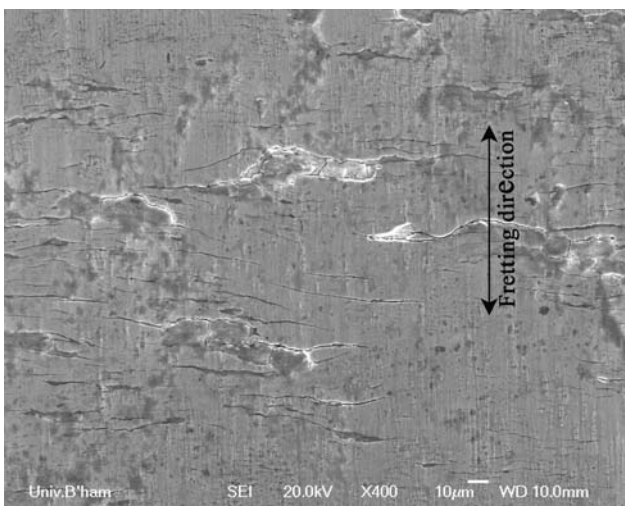

Fig. 12 SEM morphology of the central region of the 400 °C/50 h treated samples after 50,000 fretting cycles

It was reported that the nickel would be toxic for people when the released nickel concentration was higher than 9 ppm in body fluid [35]. In the present work, it has been found that under current test condition after 50,000 cycles, the maximum nickel ion concentration is only about 65 μg/L (or 0.065 ppm) for untreated NiTi, which is well below the critical value of 9 ppm. Seemingly, even the untreated NiTi will not cause a real problem. However, it should be indicated that 50,000 cycles of fretting test at a frequency of 5 Hz only takes 2.8 h, which is a short-term test. It is thus expected that the nickel ion release will increase with the fretting cycles and/or with decreasing the frequency for a given number of cycles. This is because nickel ion release during fretting corrosion is related to the synergetic attack of both mechanical fretting and chemical corrosion. Therefore, for a given number of fretting cycles, the time for corrosion in solution will increase with decreasing the frequency. Therefore, it is suggested that in order to better simulate the service conditions of NiTi body implants, fretting corrosion may need to be conducted at a relatively low frequency.

Conclusions

The fretting corrosion behaviour of the ceramic conversion treated and untreated NiTi alloy has been evaluated under gross slip fretting conditions in the simulated body fluid at room temperature. The following conclusions can be drawn from the present research.

1. The surface modified case on the 400 °C/50 h treated NiTi alloy consists of a single TiO_2 dominated layer while the 650 °C/1 h treated one has a two-layer structure: an outer TiO_2 rich layer followed by an inner Ni_3Ti rich layer.
2. All ceramic conversion treated NiTi samples can significantly reduce the nickel ion release into the simulated body fluid during fretting corrosion tests, which could be attributed to the formation of protective surface oxide layers with low nickel content.
3. The fretting damage of the un-treated NiTi is dominated by severe adhesion, cracking/delamination and abrasion in conjunction with oxidation and corrosion. Both ceramic conversion treatments can reduce the fretting damage of NiTi alloy owing to the enhanced adhesion and abrasion resistance of the surface oxide layer.

4. The fretting damage of the 650 °C/1 h treated samples is mainly caused by surface spallation because of the low bonding strength of the surface ceramic layers to the substrate and subsequently adhesion and abrasion
5. The 400 °C/50 h treated NiTi alloy possesses the best fretting corrosion properties among all three types of samples tested. The adherent surface oxide layer can effectively protect the surface from fretting damage, which is dominated by mild abrasion and oxidation.

Acknowledgements The authors are grateful for the financial support from the EPSRC, UK (GR/R09473, GR/R10974) and the Natural Science Foundation of China (50305029, 50521503). One of the authors, X. Ju, would like to thank Universities UK for an ORS Award and the Department of Metallurgy and Materials, University of Birmingham for a studentship.

References

1. T. DUERIG, A. PELTON and D. STOCKEL, *Mater. Sci. Eng.* **A273–275** (1999) 149
2. S. FUKUYO, Y. SUZUKI and E. SAIRENJI, Shape Memory Implants, in Engineering Aspects of Shape Memory Alloys, edited by T. W. DUERIG, et al., (Butterworth-Heinemann: London, Boston, Singapore, Sydney, Toronto, Wellington, 1990) p. 470
3. D. H. KOHN, *Curr. Opin. Solid State Mater. Sci.* **3** (1998) 309
4. S. A. SHABALOVSKAYA, *Bio-Med. Mater. Eng.* **12** (2002) 69
5. D. J. WEVER et al., *Biomaterials* **18**(16) (1997) 1115
6. F. TAKESHITA et al., *Biomaterials* **18** (1997) 21
7. L. M. RABBE et al., *Clin. Mater.* **15** (1994) 221
8. R.B. WATERHOUSE, Frettign wear, in ASM Handbook: Friction, lubrication and wear technology. 1992, ASM International. p. 242
9. A. W. HASSEL, *Minim. Invasive Ther. Allied Technol.* **13** (2004) 240
10. D. STAROSVETSKY and I. GOTMAN, *Biomaterials.* **22**(13) (2001) 1853
11. M. F. CHEN et al., *Mater. Sci. Eng. C* **24**(4) (2004) 497
12. S. KOBAYASHI et al., *Diamond Related Mater.* **14** (2005) 1094
13. C. M. CHAN, S. TRIGWELL and T. DUERIG, *Surf. Interf. Anal.* **15** (1990) 349
14. X.X. WANG et al., The oxide film and its effect on shape memory effect and biocompatibility in a TiNi alloy. in Shape Memory Materials'94. *Proc Inter Symp Shap. Mem. Mater.* (Beijing, China: International Academic Publishers 1994)
15. C. L. CHU, S. K. WU and Y. C. YEE, *Mater. Sci. Eng.* **A216** (1996) 193
16. G. S. FIRSTOV et al., *Biomaterials.* **23** (2002) 4863
17. B. O'BRIEN, W. M. CARROLL and M. J. KELLY, *Biomaterials.* **23**(8) (2002) 1739
18. C. H. XU et al, *Mater. Sci. Eng. A.* **371**(1–2) (2004) 45
19. C. L. CHU, C. Y. CHUNG and P. K. CHU, *Mater. Sci. Eng.* **A417** (2006) 104
20. S. A. SHABALOVSKAYA and J. W. ANDEREGG, *J. Vac. Sci. Technol.* **A13**(5) (1995) 2624
21. C. TREPANIER et al., *J. Biomed. Mater. Res. (Appl. Biomater.)* **43** (1998) 433
22. H. DONG and T. BELL, *Wear.* **238** (2000) 131
23. J. XIA et al., *Surf. Coat. Technol.* **200** (2006) 4755
24. L. TAN et al., *Mech. Mater.* **37** (2005) 1059
25. H.-H. HUANG et al., *Biomaterials.* **24**(20) (2003) 3585
26. X. JU, PhD Thesis, in Metallurgy and Materials. 2006, The University of Birmingham: Birmigham
27. L. M. QIAN, Z. ZHOU and Q. SUN, *Wear* **259** (2005) 309
28. S. J. BULL, *Tribol. Inter.* **30**(7) (1997) 491
29. Y. BERTHIER et al., *J. Tribol.* **110** (1988) 517
30. Z. R. ZHOU, L. VINCENT, *Wear* **181–183** (1995) 531
31. R. B. WATERHOUSE, *Wear.* **45** (1977) 355
32. O. VINGSBO and S. SODERBERG, *Wear* **126** (1988) 131
33. K. S. KASPRZAK, F. W. SUNDERMAN JR and K. SALNIKOW, *Mutat. Res./Fundam. Mol. Mech. Mutagen.* **533**(1) (2003) 67
34. K. SALNIKOW and E. DENKHAUS, *Crit. Rev. Oncol./Hematol.* **42**(1) (2002) 35
35. C.-C. SHIH et al., *J. Biomed. Mater. Res.* **52** (2000) 323